FEATURE ARTICLE
Attentional Functions of Parietal and Frontal Cortex

Polly V. Peers[1], Casimir J.H. Ludwig[2], Chris Rorden[3], Rhodri Cusack[1], Claudia Bonfiglioli[4], Claus Bundesen[5], Jon Driver[6], Nagui Antoun[7] and John Duncan[1]

[1]MRC Cognition and Brain Sciences Unit, Cambridge, UK, [2]Department of Experimental Psychology, University of Bristol, Bristol, UK, [3]School of Psychology, University of Nottingham, Nottingham, UK, [4]Dipartimento di Scienza della Cognizione e della Formazione, Universita degli Studi di Trento, Rovereto, Italy, [5]Department of Psychology, University of Copenhagen, Denmark, [6]Institute of Cognitive Neuroscience and Psychology Department, University College London, UK and [7]Department of Radiology, Addenbrooke's Hospital, Cambridge, UK

A model of normal attentional function, based on the concept of competitive parallel processing, is used to compare attentional deficits following parietal and frontal lobe lesions. Measurements are obtained for visual processing speed, capacity of visual short-term memory (VSTM), spatial bias (bias to left or right hemifield) and top-down control (selective attention based on task relevance). The results show important differences, but also surprising similarities, in parietal and frontal lobe patients. For processing speed and VSTM, deficits are selectively associated with parietal lesions, in particular lesions of the temporoparietal junction. We discuss explanations based on either grey matter or white matter lesions. In striking contrast, measures of attentional weighting (spatial bias and top-down control) are predicted by simple lesion volume. We suggest that attentional weights reflect competition between broadly distributed object representations. Parietal and frontal mechanisms work together, both in weighting by location and weighting by task context.

Keywords: attention, brain lesions, neuropsychology, vision

Introduction

The analysis of attentional impairments following brain lesions can be informed by a model of normal function. Here we use such a model — Bundesen's Theory of Visual Attention, or TVA (Bundesen, 1990) — to assess impairments from focal lesions of parietal and frontal cortex.

TVA is based on standard ideas of competitive parallel processing (Rumelhart, 1970). When a visual display is presented, work begins to identify the objects it contains (display elements). Though display elements are processed in parallel, the system has limited capacity; more effective processing of one element means less effective processing of others. A key factor is an element's competitive strength or attentional weight. Strong competitors are processed well, while weak competitors are processed poorly.

These ideas may be explained more formally as follows. In TVA, a central consideration is the time taken to complete identification of any display element. For each element, these identification times are exponentially distributed. For a single display element i, presented alone in the visual field, probability of identification P_i increases with processing time t according to the formula:

$$P_i = 1 - \exp(-v_i(t - t_0)) \qquad (1)$$

In this formula, v_i is the exponential rate constant or processing speed, larger values of v_i reflecting more rapid

identification. Processing time t is measured from stimulus onset; t_0 is a minimum exposure, typically of the order of 10–30 ms, required before processing can begin.

With multiple elements in the visual field, processing is competitive according to a simple rule. Each element i has an attentional weight w_i indicating how strongly it competes to be processed. For each element, processing speed is given by

$$v_i = s_i \frac{w_i}{\sum w} \qquad (2)$$

where s_i is the processing speed or v-value for element i presented alone (see Equation 1), and $\sum w$ is the sum of attentional weights for all elements in the field. Thus for a multielement display, competition is reflected in reduced processing speeds. Processing speed for each element is determined by its attentional weight relative to weights of all other elements in the field.

In TVA, completed stimulus identifications are held in a visual short-term memory (VSTM). When maintained in VSTM, a stimulus can be verbally reported or used in other conscious behavior.

Our experiments measure identification of stimuli in brief visual displays. In Part 1, we use a simple test of visual processing speed for a single display element. In Part 2, we assess attentional weights for different regions of space and for target and nontarget objects. In Part 3, we assess the capacity of VSTM.

In a previous study, we used TVA to analyze deficits in a mixed group of patients with right hemisphere lesions, generally affecting the inferior parietal lobule but extending also into frontal, temporal and occipital cortex (Duncan *et al.*, 1999). The results confirmed the importance of both processing speed and VSTM capacity; in addition to bias towards the ipsilesional side, the patients as a group showed clear deficits in both parameters. Here, we extend this work to consider more focal lesions of parietal and frontal cortex.

The concept of competitive, parallel processing in TVA is closely related to the physiological model of attention as biased competition (Desimone and Duncan, 1995; Duncan, 1996; Duncan *et al.*, 1997). In this model, inputs compete for processing in the multiple brain regions that respond to visual input. It is this competitive processing that produces limited attentional capacity. Competition is biased by such factors as sensory salience and task context (Desimone and Duncan, 1995). This bias corresponds to attentional weighting. Importantly, competition is integrated between the many visual subsystems that code different aspects of visual input. If an object

gains (or loses) strength in any one subsystem, this supports (or weakens) its processing in others. In line with behavioral data (Duncan, 1984), the result is selective processing of the same object in the many subsystems coding its different properties and implications for action. Later, we use this idea of integrated competition to consider the physiological basis for deficits in parietal and frontal patients.

Part 1: Processing Speed

To measure basic processing speed in patients and controls, we used a single, high-discriminability letter or face, presented for variable durations before a backward mask. To minimize spatial influences, this single letter or face was presented directly at fixation. v-values were estimated directly from exponential functions fit to each participant's identification data. To assess the generality of any processing speed deficit, we also administered a test of auditory choice reaction time (RT).

Materials and Methods

Participants

The total study sample comprised 36 participants, 13 with parietal lesions, 12 with frontal lesions and 11 controls (Table 1). Two frontal patients (CG and GD) were tested only in Parts 2 and 3 due to changes in their condition between test sessions. Participants were paid a small honorarium and gave full written informed consent prior to each testing session. In the parietal group (eight left, five right), some lesions extended into temporal or occipital cortex; in the frontal group (five left, seven right), lesions were strictly confined within the frontal lobe. Groups were approximately matched (Table 1) for age and premorbid IQ, assessed with the Spot-the-Word sub-test of the SCOLP (Baddeley *et al.*, 1993). To give an unbiased assessment of deficits associated with parietal and frontal lesions, patients were recruited from lesion records, without regard for behavioral impairment. Selection criteria were (i) non-traumatic unilateral lesion; (ii) age between 18 and 70 years; (iii) absence of significant current medication or psychiatric history; and (iv) normal or corrected-to-normal visual acuity (Lighthouse Near Visual Acuity Test, Lighthouse Low Vision Products, New York) and auditory acuity (assessed using a standard audiological procedure, British Society of Audiology, 1981). All patients were tested in the chronic stage (at least 6 months post-insult).

Both controls and patients were tested for clinical signs of neglect using two standard tests, the line bisection task from the BIT (Wilson *et al.*, 1987) and the Weintraub and Mesulam cancellation test (Weintraub and Mesulam, 1985). Mean deviation from the true mid-point on the bisection task is shown in Table 1, with negative scores indicating a bisection to the left of the mid-point. Two out of three bisections over 12.75 mm from the mid-point form the usual clinical cut-off for this test; only one patient (EO) and one control (RB) were found to be within the clinically significant range. Performance on the cancellation task is also shown in Table 1. Weintraub and Mesulam (1985) report the clinical cut-off on this task to be more than two errors. One control (WE), one left parietal patient (KM), two right parietal patients (BER, EO) and two right frontal patients (ET, PB) were within the clinical range. Based on these clinical assessments, neglect was weak or absent in our patients.

Lesion Analysis

Structural MRI scans of all patients' brains were acquired on a 1.5 T scanner (T1-weighted SPGR, 3-D, resolution 0.98 × 2 × 0.98 mm, whole brain coverage). Lesions were traced on contiguous slices by a neurologist using the MRIcro (Rorden and Brett, 2000). Brains were normalized to a space of the Montreal Neurological Institute (MNI) template using SPM99 (http://www.fil.ion.ucl.ac.uk/spm), with affine plus non-linear transforms and cost function masking as described by Brett *et al.* (2001). After normalization, MATLAB (Mathworks) routines were used to calculate each lesion's center of mass, defined by mean MNI x (left–right), y (posterior–anterior) and z (inferior–superior) coordinates of

Table 1

Participant details: demographic data, medical history and performance on standard tests of word recognition and unilateral neglect

Participant	Age (years)	Sex	Etiology[a]	Time from onset to first testing (months)	Spot-the-word (correct/60)	Line bisection error (mm)[b]	Cancellation (omissions/60)
Control							
AB	55	M			51	1.3	0
AJ	57	F			55	−3.0	0
BBD	47	F			56	−3.5	0
BR	65	M			50	−2.3	0
CH	58	M			48	3.0	0
CS	59	F			45	−0.3	0
HG	48	M			52	−6.8	0
JAM	40	F			54	−0.2	0
RB	50	M			54	−14.8	0
RO	50	M			47	3.8	0
WE	63	F			55	−3.5	4
Mean	54				52	−2.4	0.4
Left parietal							
AMO	37	F	meningioma	20	50	−1.0	0
BT	70	M	infarct	61	48	−3.5	2
IH	50	F	meningioma	113	56	0.8	0
JAL	52	M	infarct	59	47	−3.0	0
JEL	51	F	meningioma	42	54	−2.0	2
KM	67	M	meningioma	9	59	−7.7	4
PD	49	M	meningioma	26	47	−3.8	0
SB	45	M	infarct	84	45	3.2	0
Mean	53			52	51	−2.1	1.0
Right parietal							
BER	63	F	aneurysm	6	51	5.8	4
EO	62	M	aneurysm	52	41	11.0	10
MB	43	F	infantile CVA	504	46	10.2	0
MIB	54	M	infarct	8	57	−9.8	0
RC	69	M	infarct	18	56	−1.8	1
Mean	58			118	50	3.1	3.0
Left frontal							
AD	64	F	infarct	48	54	−4.3	2
GD	47	F	oligodendroglioma	180	54	−3.7	0
PAP	60	F	meningioma	29	52	−6.8	2
PM	47	M	meningioma	20	53	7.7	0
US	52	F	heamangioma	33	56	−4.8	0
Mean	54			62	54	−2.4	0.8
Right frontal							
CE	65	M	aneurysm	25	53	−4.5	0
CG	52	F	oligodendroglioma	420	52	5.0	2
DT	69	M	infarct	38	58	−7.3	0
ET	49	F	aneurysm	40	58	6.0	3
MS	70	M	infarct	29	58	−6.3	0
PB	54	F	meningioma	19	39	−5.2	3
SS	47	F	oligodendroglioma	54	47	−3.7	0
Mean	58			85	52	−2.3	1.1

[a]All tumor patients had undergone surgical resection; patients with aneurysms had undergone surgery following vessel rupture.
[b]Mean error from true midpoint in three bisections of lines 205 mm in length (−ve left, +ve right).

included voxels, along with total lesion volume. Normalized brains and lesions are shown in Figures 1 (parietal) and 2 (frontal).

Processing Speed

Testing was carried out on a Dell Inspiron 370 laptop computer connected to a 17″ Dell Trinitron monitor. Participants sat in a comfortable position ~50 cm from the screen; as viewing distance was not controlled precisely, reported visual angles are approximate.

The main experiment (controls and both patient groups) measured letter processing. Trials commenced with a procedure designed to ensure central fixation. A red fixation cross (1.2 × 1.7°) presented on a grey background appeared at screen center (see Fig. 3A). When the experimenter pressed a key, the cross flashed on and off three times over a period of 600 ms, before being replaced by a small red digit (0.6 × 0.8°) for 150 ms. A static red cross reappeared in the center of the screen and participants were requested to report the identity of the digit. This task was not scored, but the trial was abandoned if no digit
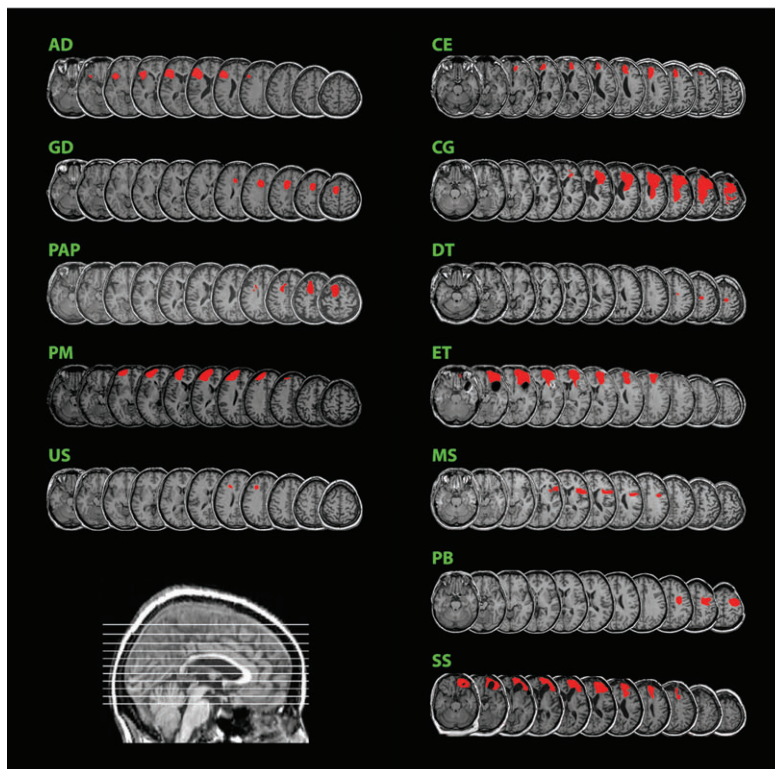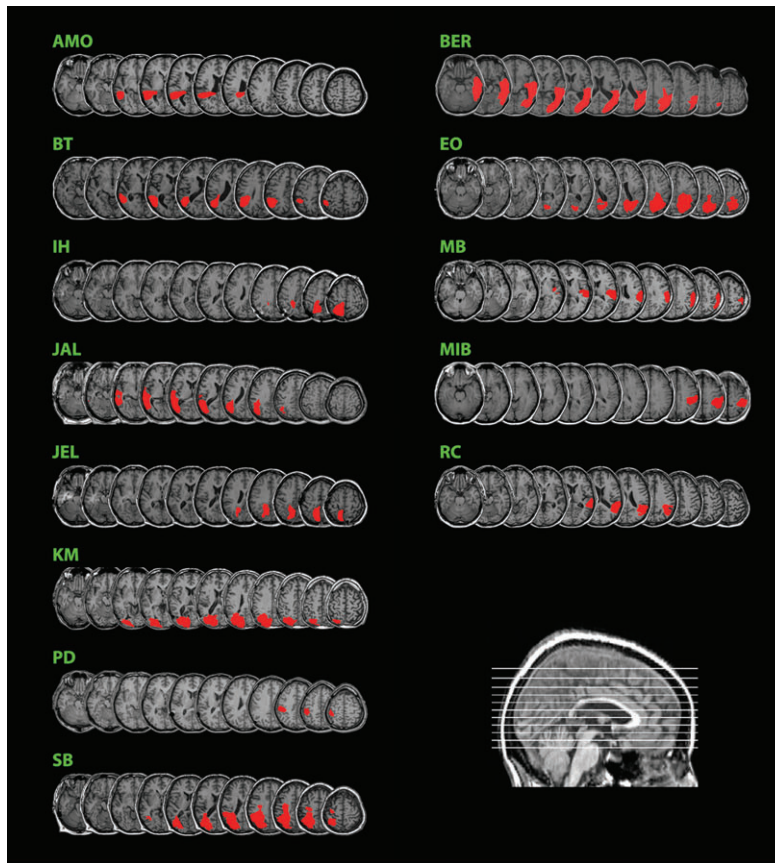
Figure 1. Parietal group lesion drawings. Each patient's lesion is shown in red on a structural MRI of their own brain, normalized using SPM99 to MNI space. For each patient, axial slices (left hemisphere to the left) are shown at MNI z-levels of -24, -16, -8, 0, 8, 16, 24, 32, 40, 50, and 60 mm (indicated on sagittal midline slice at bottom right of figure). There are eight patients with left hemisphere lesions (left column) and five with right hemisphere lesions (right column).

Figure 2. Frontal group lesion drawings. Conventions as Figure 1. There are five patients with left hemisphere lesions (left column) and seven with right hemisphere lesions (right column).

could be reported. Failure to report the digit occurred only for two trials in one participant.

A second keypress from the experimenter initiated the main task. The cross flashed as before, this time to be replaced by a black target letter (2.9 × 5°). Letters were upper case, randomly picked from the set BCDFGHJKLNPQRSTVXYZ. Letters were presented for one of five exposure durations (23, 46, 80, 114 and 171 ms, selected to cover the full accuracy range), and were immediately replaced by a pattern mask of the same size, consisting of jumbled letter features, presented for 200 ms. Participants were requested to report the identity of the target. They were told to respond only if they were fairly confident of what they had seen. The experimenter entered the response into the computer before initiating the next trial. There were 48 trials at each exposure duration, mixed in a random order over six experimental blocks. To reduce tiredness, rest periods and other standard clinical tests were given between blocks.

For controls and parietal patients only, the generality of the results was tested with a second set of stimuli. This experiment used faces instead of letters. Face and letter experiments were run in separate sessions. In the face experiment the fixation task was not used; instead each trial simply began with a static fixation point. Faces (6.5 × 6.5°) consisted of 12 black and white photos of famous people, all of them familiar to all participants. Faces were presented for one of five exposure durations (12, 24, 47, 82 and 118 ms), and were immediately replaced by a pattern mask of the same size, comprising all 12 faces superimposed. In other respects, face and letter experiments were similar.
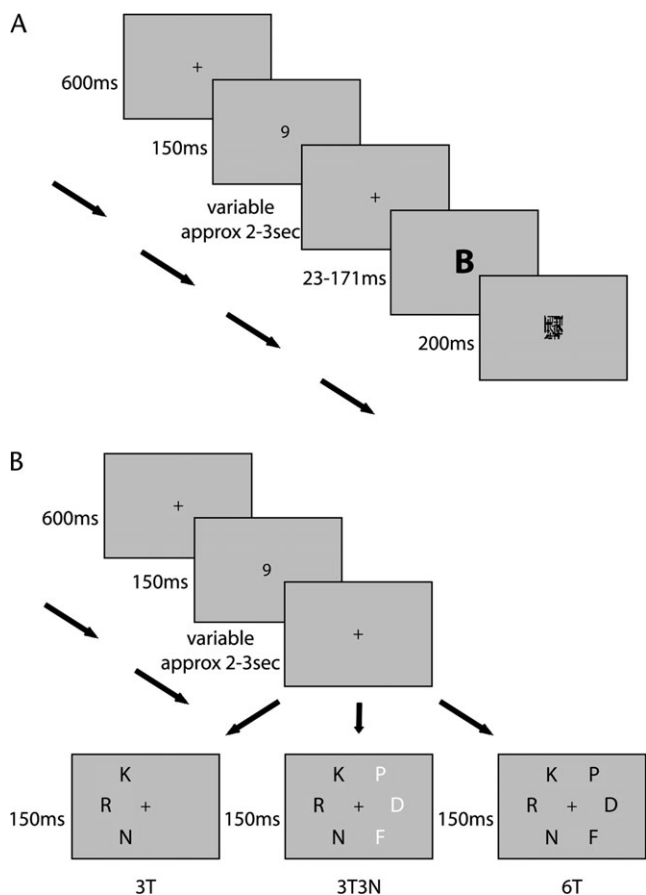

Figure 3. Diagrammatic representations of the experimental tasks. (A) Example trial of the single letter processing task. The first task on each trial was identify an unmasked digit. This task was included simply to ensure central fixation and was not scored. The second task was to identify a masked letter. (B) Example trials of the partial report task. The first task was unscored as before; the second task was to identify letters in a specified target color (here black), each display containing three targets (in either left or right hemifield, 3T), six targets (three on each side, 6T) or three targets in one hemifield with three different-color nontargets on the opposite side (3T3N).

Auditory Choice RT
In the choice RT task, participants were asked to respond as quickly and accurately as possible to low (frequency 200 Hz) and high (frequency 4000 Hz) pure tones, presented binaurally for 200 ms over Sennheiser HD 250 linear II headphones. Responses were made by pressing either the left (low tones) or the right (high tones) button of a serial mouse. The interval from response to the following stimulus was randomized between 500 and 995 ms. Each participant carried out one practice block of 24 trials, then four experimental blocks of 24 trials each. Rests were taken between blocks.

Results

Processing Speed
To illustrate the range of performance, Figure 4 shows data for three individual participants. These data come from the letter task, showing proportion of correct letter identifications as a function of exposure duration. Participants illustrated in Figure 4 are the slowest (lowest v_i) parietal and frontal patients compared with the median control. Separately for letter and face tasks, best fits to each participant's data were obtained using equation (1) (Fig. 4, solid lines). Values of v_i for all participants appear in Table 2.

Parietal Patients. Parietal deficits in v_i were assessed by analysis of variance (ANOVA). A first analysis, dealing only with patients, had the factors group (left versus right lesions) and stimulus type (letter versus face). There was no significant effect of group [$F(1,11)$ = 0.69] and no group by stimulus type interaction [$F(1,11)$ = 0.77]. For comparison with controls, accordingly, left and right patients were combined. Distributions of v_i scores are shown in Figure 5, separately for letters and faces, for controls (Fig. 5A,D) and combined parietal patients (Fig. 5B,E). An ANOVA on mean v_i scores across stimulus types showed parietal patients were significantly slowed relative to controls [$F(1,22)$ = 8.77, $P < 0.01$].

Figure 6A contrasts lesion locations of the four patients with the lowest (most impaired; upper row) and highest (least impaired; lower row) mean v_i scores. To facilitate assessment of lesion overlap irrespective of side, right-sided lesions have been transposed onto the left hemisphere. The figure suggests a separation between most and least impaired patients. For the most impaired patients, lesions are relatively inferior, centering around the temporo-parietal junction (TPJ). For the least
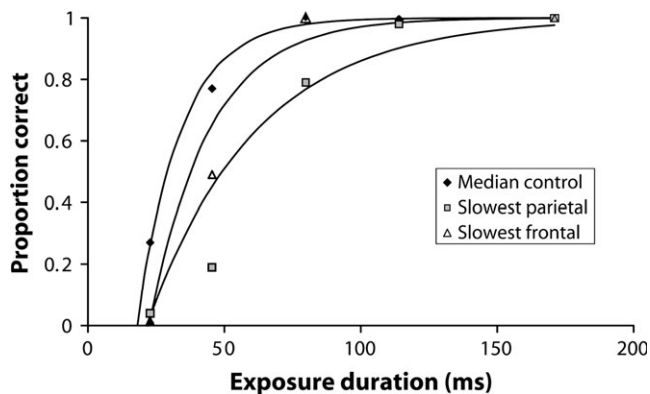

Figure 4. Data for three illustrative participants in the single letter task. The slowest (lowest v_i) patients from parietal (JA, grey squares) and frontal (MS, white triangles) groups are compared with the median control (HG, black diamonds). For each participant, solid curve shows theoretical fit to the data by equation (1).

Table 2
Parameter estimates for each participant

Participant	v_i letters (letters/s)	v_i faces (faces/s)	Bias[a]	α'	K'
Control					
AB	52.0	66.0	0.40	1.12	4.2
AJ	57.0	86.0	0.48	0.96	4.2
BBD	111.8	74.1	0.52	0.92	4.5
BR	71.7	35.1	0.49	0.86	4.1
CH	63.6	32.0	0.51	0.99	3.5
CS	62.4	45.5	0.42	0.87	4.5
HG	62.9	39.3	0.53	0.92	4.3
JAM	125.0	75.0	0.45	0.90	4.5
RB	144.3	26.4	0.48	0.95	5.5
RO	59.8	60.6	0.46	1.00	3.4
WE	40.5	37.5	0.43	0.95	4.2
Mean	77.4	61.6	0.47	0.95	4.3
Left parietal					
AMO	35.4	37.2	0.45	1.06	2.4
BT	41.7	41.6	0.49	1.17	3.4
IH	79.0	59.5	0.31	0.95	4.3
JAL	25.1	35.0	0.64	0.98	2.6
JEL	49.8	56.8	0.54	0.97	3.5
KM	37.5	45.7	0.63	1.17	2.3
PD	52.3	38.7	0.57	0.81	3.4
SB	54.2	44.2	0.86	1.11	2.1
Mean	46.9	44.8	0.56	1.03	3.0
Right parietal					
BER	38.8	19.9	0	1.05	3.1
EO	42.7	37.0	0.04	1.10	2.7
MB	58.4	56.4	0.25	0.94	2.6
MIB	35.6	38.3	0.55	0.92	5.3
RC	44.7	33.0	0.31	0.88	3.2
Mean	44.0	36.9	0.23	0.98	3.4
Left frontal					
AD	57.7	–	0.46	0.99	3.5
GD	–	–	0.55	0.94	5.3
PAP	47.2	–	0.65	0.99	2.3
PM	61.4	–	0.47	0.92	4.5
US	49.4	–	0.47	0.87	5.3
Mean	53.9		0.52	0.93	4.2
Right frontal					
CE	57.5	–	0.81	0.92	2.1
CG	–	–	0.09	1.02	3.3
DT	58.7	–	0.47	0.88	3.3
ET	76.5	–	0.32	0.98	4.3
MS	45.7	–	0.21	0.79	2.8
PB	48.9	–	0.45	0.94	2.1
SS	101.3	–	0.30	0.98	4.3
Mean	64.8		0.38	0.94	3.2

[a]Scores <0.5 show bias to right; scores >0.5 show bias to left.

impaired patients, in contrast, lesions center in the superior parietal lobule. Across the whole patient group, there was a substantial correlation ($R^2 = 0.48$, $P < 0.01$) between the z-level of the lesion's center of mass and the mean v_i score (Fig. 6B). Simple lesion volume, in contrast, was unpredictive ($R^2 = 0.14$, Fig. 6C).

To summarize, parietal patients as a group showed a significant impairment in processing speed. More specifically, this impairment was associated with inferior lesions, in the general region of the TPJ.

Frontal Patients. The distribution of v_i scores in frontal patients (letter task only) appears in Figure 5C. Comparison with controls (Fig. 5A) suggests little reduction in processing speed as a result of frontal lesions. An initial ANOVA showed no significant difference between left and right hemisphere patients [$F(1,10) = 0.91$]. A second ANOVA contrasting controls with all frontal patients also showed no significant difference [$F(1,21) = 2.25$]. Finally, the group of combined frontal patients showed significantly higher v_i scores than the group of combined parietal patients [$F(1,23) = 5.97$, $P < 0.05$].

In the frontal group, there was a significant positive correlation between v_i scores and lesion volume ($R^2 = 0.76$, $P < 0.01$), with faster processing apparently associated with larger lesions. On closer examination, this correlation derived largely from the two patients with the largest lesions. Accompanying their high v_i scores, these patients showed high rates of false identifications, suggesting relatively unconservative responding.

To summarize, any processing speed deficit in frontal patients was modest, and not significant in the group as a whole.

Supplementary Lesion Analyses. In some parietal patients, lesions spread into occipitotemporal cortex. Supplementary analyses assessed the importance of this damage for deficits in v_i. A first analysis measured total volume of occipital damage by summing the volumes of damage in calcarine, superior occipital, middle occipital and inferior occipital regions described in the AAL maps (http://www.psychology.nottingham.ac.uk/staff/cr1/template.html; Tzourio-Mazoyer *et al.*, 2002). Total occipital lesion volume did not correlate with v_i ($R^2 = 0.07$). Given their importance in visual shape recognition, including recognition of faces (Kanwisher *et al.*, 1997) and words (Cohen *et al.*, 2002), we separately assessed damage to fusiform cortex and the lateral occipital complex. Only four patients had damage to these areas (defined as fusiform and inferior occipital cortex in the AAL maps). Lesion volume in this region showed no significant correlation with v_i ($R^2 = 0.15$).

Auditory RT
Mean auditory RT was 381 ms for controls, 443 and 528 ms respectively for left and right parietal patients, and 547 and 531 ms respectively for left and right frontal patients. Both combined parietal [$F(1,22) = 8.77$, $P < 0.01$], and combined frontal [$F(1,21) = 11.53$, $P < 0.01$] groups were significantly slower than controls. Thus auditory RT shows a quite different pattern of impairment from visual processing speed, with the worst performance in frontal lobe patients. In the parietal group, there was no significant correlation between auditory RT and v_i score ($R^2 = 0.15$) or between auditory RT and lesion z-level ($R^2 = 0.01$).

Discussion
We measured visual processing speed for a single letter or face, presented for variable durations at fixation. No significant impairment was found in patients with frontal lesions. In the parietal group, slowed processing was specifically associated with lesions in the region of the TPJ.

As a basic measure of processing efficiency, speed will certainly be influenced by the integrity of sensory and pattern recognition processes. Neuroimaging results implicate a set of ventral occipital and occipitotemporal regions in recognition of patterns and objects, including the lateral occipital complex (Corbetta *et al.*, 1990; Malach *et al.*, 1995), visual word form area (Cohen *et al.*, 2002) and fusiform face area (Kanwisher *et al.*, 1997). As we should expect, we previously observed reduced processing speed for letters in association with a left occipital lesion and 'ventral simultanagnosia' (Duncan *et al.*, 2003). In the present patients, however, ventral occipitotemporal damage was rare, and unable to account for sharp reductions in processing speed. Instead, the data show that
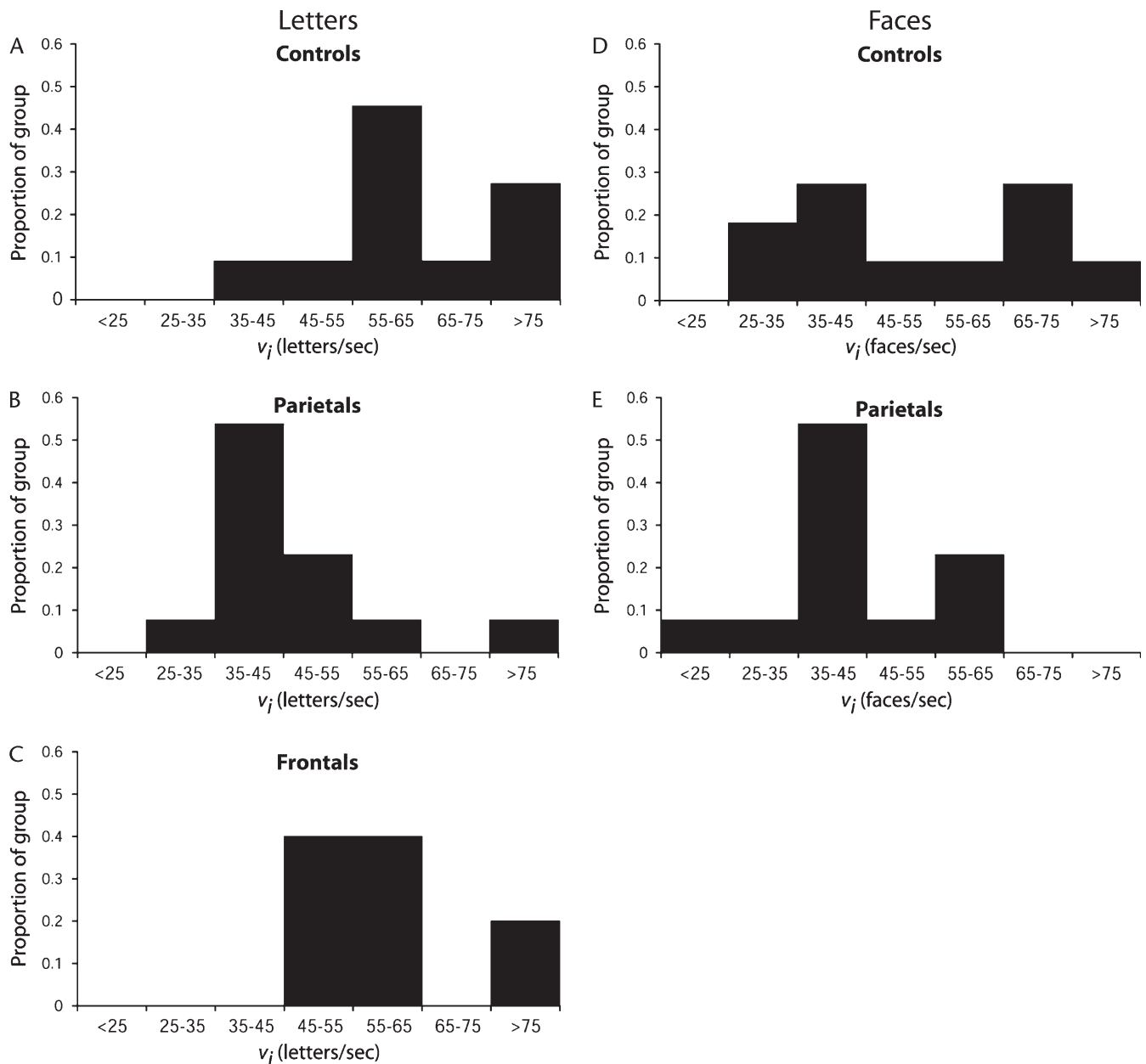
Figure 5. Distributions of the v_i parameter for both letters and faces for control participants (*A* letters, *D* faces) patients with parietal lesions (*B* letters, *E* faces) and patients with frontal lobe lesions (*C* letters). Lower values of v_i indicate slower visual processing.

processing speed is also strongly influenced by more dorsal lesions, in the region of the TPJ.

One possibility is that lesion results reflect the functions of TPJ cortex. This cortex may play some important role in construction of a reportable, conscious visual percept. Recent imaging data show TPJ activation in association with target (Linden *et al.*, 1999; Marois *et al.*, 2000; Downar *et al.*, 2001), occasional (Downar *et al.*, 2000) or unexpected (Corbetta *et al.*, 2000) events in a stream of visual, auditory or tactile stimuli. In event-related potential (ERP) studies, TPJ lesions have been shown to reduce the P300 response, conventionally associated with stimulus identification and update of working memory (Soltani and Knight, 2000) — though certainly the P300 is a complex component with multiple neural generators (Soltani and Knight, 2000). Together, these data have been interpreted

in terms of a role for TPJ in identification and awareness of multimodal stimulus input (Downar *et al.*, 2000, 2001).

A second hypothesis, however, is also worth considering. It is sometimes suggested that attentional deficits after parietal lesions may be more associated with white matter than grey matter damage (Gaffan and Hornak, 1997; Samuelsson *et al.*, 1997). In the monkey, for example, Gaffan and Hornak (1997) found major spatial bias associated not with unilateral removal of parietal cortex on one side, but with unilateral section of white matter beneath the intraparietal sulcus. Major white matter tracts connecting posterior and anterior brain regions pass behind the posterior end of the lateral sulcus, suggesting that a TPJ lesion could produce a substantial disruption of intrahemispheric communication. As discussed above, a central proposal in the biased competition model is that 'attention' to
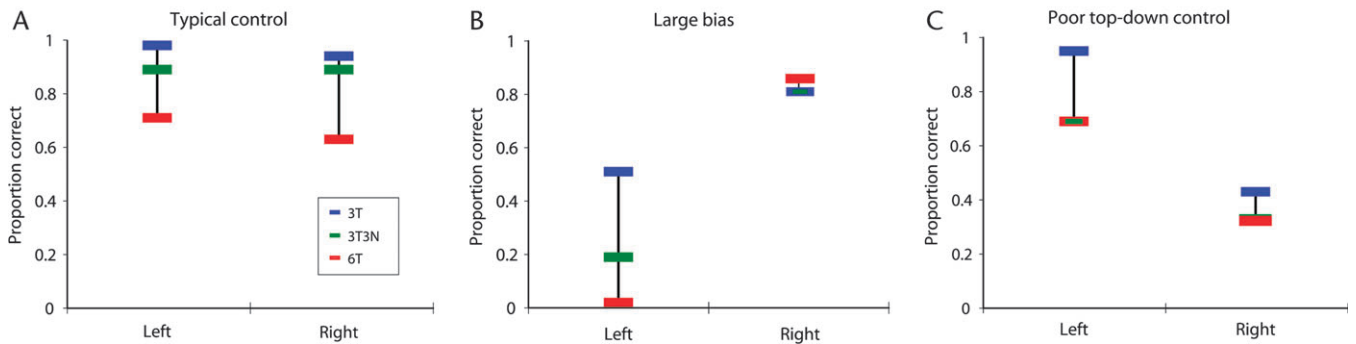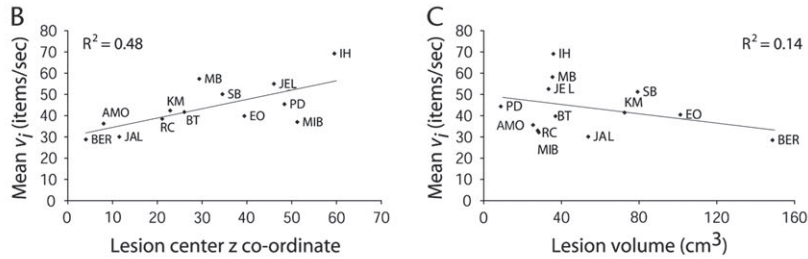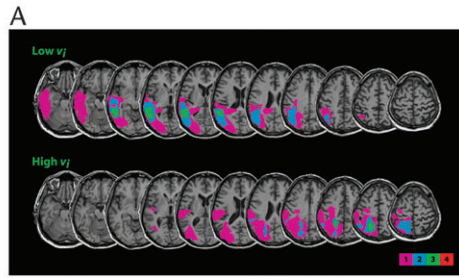
Figure 6. Processing speed in parietal patients. (*A*) Lesion overlay diagrams of the four slowest (lowest mean v_i; upper panel) and the four fastest (highest mean v_i; lower panel) patients. Right hemisphere lesions have been transposed so that all lesions appear on the left hemisphere. There are three left and one right hemisphere lesion patients in both the 'slowest' and 'fastest' groups. Slice selection as Figure 1. Purple, blue, green and red indicate regions damaged in respectively 1, 2, 3 and 4 patients. (*B*) Relationship between mean v_i and z coordinate of lesion center of mass. (*C*) Relationship between mean v_i and lesion volume.

Figure 7. Data for 3 illustrative participants in partial report task. Proportions of letters identified in left and right visual fields, separately for 3T (blue), 6T (red) and 3T3N (green) displays. (*A*) Typical control (BBD). (*B*) Patient with strong spatial bias (parietal lesion, EO). (*C*) Patient with poor top-down control (parietal lesion, BT).

an object develops through reciprocal interaction between the multiple cortical and subcortical regions coding this object's properties and action implications (Duncan, 1996; Duncan *et al.*, 1997). Recent imaging data, too, show that detected and undetected visual events differ not just in visual system activation, but in broad recruitment of parietal and prefrontal cortex when conscious detection takes place (Beck *et al.*, 2001). Plausibly, white matter lesions around the TPJ could produce serious disturbance in a process of integrating cortical function to the end of conscious perception.

One question addressed by our data concerns the generality of the speed deficit associated with TPJ lesions. In contrast to visual *v*-values, auditory choice RTs were not selectively impaired by TPJ lesions. Instead, RTs were increased in both parietal and frontal lesion groups, with the largest deficits in frontal patients. One possibility is that TPJ lesions are specifically associated with slowed processing in the visual modality. Perhaps more likely, however, is an important difference between measures of perceptual processing, based on brief stimulus presentations, and measures of speeded response production, based on choice RT. In addition to stimulus identification, choice RT incorporates important stages of response selection and execution (Sternberg, 1969). RT is strongly influenced, for example, by the rule mapping stimulus to response alternatives (Fitts and Deininger, 1954). At this stage, the most probable conclusion is that speed deficits associated with TPJ lesions concern specifically the speed of stimulus identification; and that in the auditory RT task, any contribution of stimulus identification time is modest by comparison with response selection time.

Part 2: Attentional Allocation

In Part 2 we turn to attentional allocation, determined in TVA by attentional weights. We use brief multiletter displays. In such a display, processing speeds (and hence the probability of letter identification) are determined by equation (2). Strong competitors (high attentional weight) are processed relatively well, and interfere strongly with others. Weak competitors (low attentional weight) are processed poorly, and interfere weakly with others.

Our experiment is a variant of the partial report task (Sperling, 1960; Bundesen, 1990). Participants see brief displays of three or six letters (Fig. 3*B*). Letters can be black or white; either

black letters are targets and white letters nontargets, or vice versa. The task is to identify as many targets as possible. On different trials, the display consists of (i) three target letters (3T), either in left or right visual field; (ii) six target letters (6T), three in each field; or (iii) three targets in one field accompanied by three nontargets in the other (3T3N). Scores are proportions of letters correctly identified. The task is used to measure spatial bias — attentional allocation to left versus right visual field — and top-down control — allocation to targets versus nontargets.

Spatial bias is closely related to the clinical phenomenon of unilateral extinction. In extinction, a single stimulus is detected or identified relatively well in either left or right hemifield. For one side, however — usually the side opposite to a unilateral lesion — performance is strongly impaired when left and right stimuli appear together. Such data are well explained by the proposal that simultaneous inputs compete for attention, with strong bias towards one (usually the ipsilesional) side (Ward et al., 1994). Such a bias would have no effect in a unilateral display, but a strong effect in a bilateral display.

In line with this, TVA captures spatial bias by differential attentional weighting for left and right hemifields. In our study, as in extinction, bias is measured by comparing unilateral and bilateral displays. Specifically, we examine loss of performance in the 6T display (bilateral) as compared with the 3T displays (unilateral). In principle, proportion correct scores for 3T and 6T displays can be combined with equations (1) and (2) to derive estimates of attentional weights on the two sides (Duncan et al., 1999). Whichever side shows better preserved performance in the 6T display will be assigned a greater attentional weight, and a natural measure of spatial bias is

$$\frac{w_L}{w_L + w_R} \qquad (3)$$

where w_L is the attentional weight of elements in the left field, while w_R is the weight of elements in the right field. A ratio close to 0 indicates strong bias to the right, with good right-side performance in the 6T display. A ratio close to 1 means strong bias to the left, with good left-side performance.

In practice we can use a simpler score which gives closely similar results (Duncan et al., 1999). For each side, we define a maintenance score showing how well performance is preserved in the 6T display. For the left, this score M_L is defined as proportion correct for left field letters in the 6T display, divided by proportion correct for the same letters in a left-field 3T display. M_R is defined equivalently for the right. Then spatial bias is measured as

$$\frac{M_L}{M_L + M_R} \qquad (4)$$

Again, a score close to 0 indicates strong bias to the right, while a score close to 1 indicates strong bias to the left.

Our second measure concerns top-down control, or focus of attention on task-relevant letters. How should attentional weights be set in partial report? Ideally, targets should have high weights and be processed well. Nontargets should have low weights and be processed little. In our task top-down control is assessed by comparing the three display types defined above, specifically display 3T3N with 3T and 6T displays. In the best case (perfect top-down control), attentional weights would be perfectly controlled by task relevance. Negligible weight for nontargets would mean that all processing in the 3T3N display was directed to targets. Subjectively, targets would be attended

and nontargets would be ignored. Performance would be equal in displays 3T3N and 3T. In the worst case (no top-down control), attentional weights would be independent of task context. Equal weight for targets and nontargets would mean that performance was equal in displays 3T3N and 6T. Subjectively, attention would be paid equally to targets and nontargets. In general, performance for the 3T3N display will move between two bounds, an upper bound established by the 3T display and a lower bound established by the 6T display. Where performance actually lies reflects the efficiency of top-down control. In practice, it varies widely depending on the variant of partial report used (e.g. selection by target luminance, as here, versus selection by location, alphanumeric category etc.; see Bundesen, 1990; Bundesen et al., 1985).

In principle, top-down control can be measured by fitting TVA quantitatively to the data, and estimating attentional weights separately for targets and nontargets. A natural measure of control is α, defined as

$$\alpha = \frac{w_N}{w_T} \qquad (5)$$

where w_N is the mean attentional weight of a nontarget and w_T is the mean attentional weight of a target (Bundesen, 1990). A value of zero indicates perfect top-down control, while a value of one indicates no control. In practice, we use a simpler score directly reflecting where performance in the 3T3N display lies between its upper and lower bounds. Let P_{3T} be the mean probability correct for the 3T display, P_{6T} the probability correct for the 6T display, and P_{3T3N} the probability correct for the 3T3N display. Then the control parameter α′ is defined as:

$$\alpha' = \frac{P_{3T} + P_{6T}}{2P_{3T3N}} \qquad (6)$$

As for α, higher values reflect poorer top-down control. Previously, we have shown α and α′ to be strongly correlated (Duncan et al., 1999).

Materials and Methods

Participants
Participants were the full set of 36 described in Part 1.

Partial Reports
The partial report task used multi-letter arrays, always shown for 150 ms and without a backward mask (see Fig. 3B). The task was to report just letters of a particular color (either black or white). Starting target color was randomized across individuals, with all subjects completing two blocks of trials with targets in one color before swapping target color for the remaining two blocks.

Eye movements were monitored using an ASL 310 eye-tracker (Applied Science Laboratories, Bedford, MA). The eye tracker sensors were attached to a pair of optical frames, allowing acuity deficits to be corrected with optician's lenses. For this purpose, participants' own spectacle correction was measured (LM-350 Lensmeter, Nidek Ltd, Japan) and copied. At the beginning of each task block, the eye monitor was calibrated using fixations at screen center and 10° to right and left. In all other respects equipment, general experimental conditions, and initial fixation task on each trial were the same as those used in the single letter task described in Part 1. Letters for each array were selected without replacement from the same set as before.

The target array for each trial was randomly picked from one of five experimental conditions. These were: (i) three letters (3.3 × 5°) in the target colour appearing in the left visual field (3T-left). These formed a semicircular configuration centered 11.6° from the fixation cross, with

the middle letter on the horizontal meridian and the other two letters at angles of 50° above and below. (ii) Three letters in the target colour appearing in the same spatial arrangement in the right visual field (3T-right). (iii) Combination of arrays (i) and (ii) to give six letters in the target colour, three in each visual field (6T). (iv) Three letters in the target colour appearing in the left visual field, with three letters in the nontarget color in the right visual field (3T3N-left). (v) Three letters in the target colour appearing in the right visual field, with three letters in the nontarget color in the left visual field (3T3N-right).

On each trial participants were requested to report as many target letters as possible. Trials were excluded if a horizontal eye movement of >1.9° was detected between initial fixation and mask onset. Participants completed four blocks of 40 trials, providing a maximum of 32 trials in each of the conditions. Breaks were taken between blocks.

Results

Data from three illustrative participants appear in Figure 7. Values are proportion of letters correctly identified, separately for left and right visual fields, and for 3T (blue), 6T (red) and 3T3N (green) displays. The typical control (Fig. 7A) shows the expected results: performance is best for 3T, worst for 6T and intermediate for 3T3N. Figure 7B shows a patient with strong spatial bias: the 6T display is associated with very poor performance in the left hemifield, but preserved performance on the right. Figure 7C shows a patient with poor top-down control: performance for each hemifield is the same whether the opposite hemifield contains targets (6T, red) or nontargets (3T3N, green).

Spatial Bias

Parietal Patients. For each participant, a spatial bias score was calculated by equation (4) (see Table 2). Bias score distributions appear in Figure 8. For controls (Fig. 8A), the distribution is strongly peaked around 0.5, indicating similar attentional weighting of the two sides. For left and right parietal patients (Fig. 8B,C), distributions are more broadly spread. As anticipated, left patients show attentional bias to the left, indicating relatively poor identification of right field letters in the bilateral display. Right patients show a complementary attentional bias to the right. Also worth noting is a single left patient (IH) with paradoxical bias, to the right rather than the left.

As a measure of bias independent of direction, for each participant we took the absolute difference of the obtained
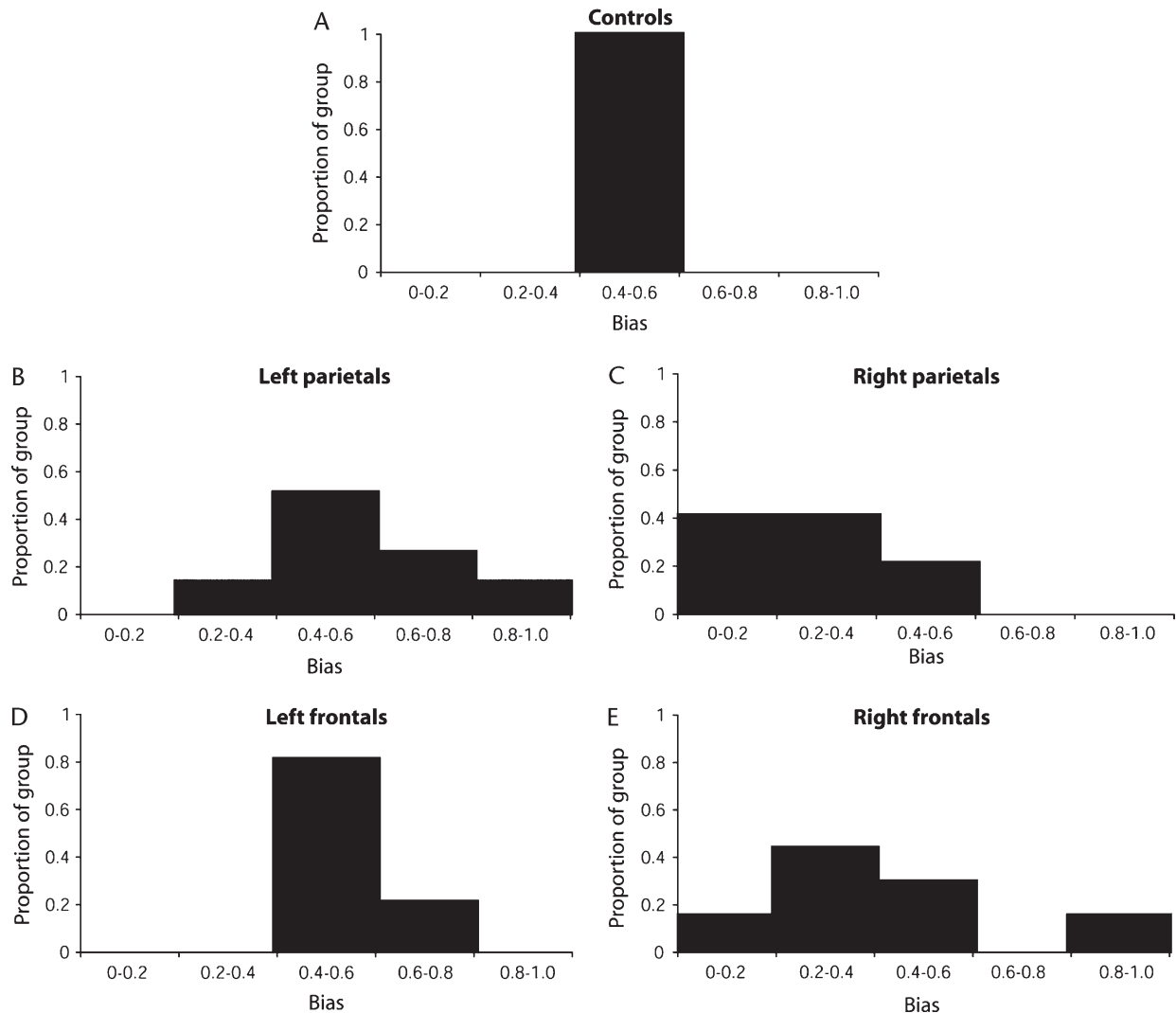

Figure 8. Distributions of spatial bias for (A) controls, (B) left parietals, (C) right parietals, (D) left frontals and (E) right frontals. Values <0.5 indicate bias to the left, while values >0.5 indicate bias to the right.

score from an unbiased value of 0.5. An ANOVA contrasting left and right parietal patients showed a near significant difference [$F_{(1,11)} = 4.05$, $P = 0.07$], whose interpretation we shall return to below. Given generally similar results in left and right patients, however, we combined them for a single comparison between parietal patients and controls. Absolute bias was significantly greater in the parietal group [$F_{(1,19)} = 6.50$, $P < 0.05$].

Figure 9*A* contrasts the four patients with largest (upper row) and smallest (lower row) absolute bias. Again, right hemisphere lesions have been reflected such that all lesions appear on the left. Unlike the results for processing speed (Fig. 6*A*), the impression is that distributions of lesion location are rather similar for most and least biased patients. The more biased patients, however, appear to have larger lesions overall. Regression analysis confirmed these conclusions. In the combined parietal group, absolute bias was independent of *z*-level ($R^2 = 0.04$; Fig. 9*B*), but significantly correlated with lesion volume ($R^2 = 0.70$, $P < 0.01$; Fig. 9*C*). This effect of lesion volume, indeed, accounts for the tendency (above) for stronger bias in right hemisphere patients. An ANCOVA comparing left and right patients with volume covaried showed no significant difference between sides [$F_{(1,10)} = 2.99$].

To summarize, both left and right parietal lesions produced lateral attentional bias. In most cases, bias was to the ipsilesional side. The strength of bias was predicted not by the site of lesion within parietal cortex, but by simple lesion volume.

Frontal Patients. Bias distributions for frontal lobe patients appear in Figure 8*D,E* (left and right patients respectively). Again, the tendency is for bias to the ipsilesional side, though one right hemisphere patient (CE) shows paradoxical bias to the left. Comparison of absolute bias in left and right frontal groups showed a marginally significant difference [$F_{(1,10)} = 5.22$, $P = 0.05$]. Again this difference between left and right patients disappeared in an ANCOVA covarying lesion size [$F_{(1,10)} = 2.47$]. In a further analysis, combined left and right frontal patients showed significantly stronger bias than controls [$F_{(1,18)} = 5.21$, $P < 0.05$].

A comparison of most and least biased frontal patients (Fig. 10*A*) again suggests that more biased patients simply had larger lesions. The conclusion is confirmed by regression analysis ($R^2 = 0.42$, $P < 0.05$; Fig. 10*B*).

To summarize, bias results for frontal patients were closely similar to those of the parietal group. Frontal lesions increased spatial bias, usually towards the ipsilesional side. Bias was predicted not by lesion location within frontal cortex, but by simple lesion volume.

Supplementary Lesion Analyses. Further analyses addressed relations between spatial bias and damage to specific subregions of parietal and frontal cortex. Based on the MNI single subject template brain, regions of interest (ROIs) were defined for the intraparietal sulcus (IPS), frontal eye field (FEF) and dorsolateral prefrontal cortex (DLPFC). In parietal patients, volume of IPS damage was quite strongly correlated with total lesion volume ($R^2 = 0.42$, $P < 0.01$). Nevertheless, it was a worse predictor of spatial bias ($R^2 = 0.36$ versus $R^2 = 0.70$). In the frontal lobe, there were only three patients with FEF lesions and three with DLPFC lesions. In neither case did these patients show obvious differences from the remainder of the frontal group.

Top-down Control
Initial analyses showed that, both for parietal and frontal patients, top-down control parameters (equation 6) were similar for targets in the two hemifields. For every participant, accordingly, mean values of P_{3T}, P_{6T} and P_{3T3N} (see equation 6) were calculated across left and right hemifields, and entered into equation (6) to produce an overall value of α' for the two sides combined (see Table 2). Initial analyses also showed no significant difference between patients with left and right hemisphere lesions, who were accordingly combined.

ANOVAs of α' values showed no significant difference, either between parietal patients and controls [$F_{(1,23)} = 2.22$] or between frontal patients and controls [$F_{(1,21)} = 0.24$]. In both groups, however, there was a significant correlation between α' and lesion volume (parietal patients, $R^2 = 0.29$, $P < 0.05$; frontal patients, $R^2 = 0.43$, $P < 0.01$). As for spatial bias, parietal data showed no significant correlation between α' and lesion *z*-level ($R^2 = 0.15$). As parietal and frontal groups showed similar effects of lesion volume, they were combined for a further analysis. By median split, the combined group was divided into large and small lesion sub-groups, and these were entered into a one-way ANOVA comparing large-lesion, small-lesion and control participants. The analysis revealed a significant effect of group [$F_{(2,33)} = 8.00$, $P < 0.01$]. Post-hoc analyses showed that patients with large lesions differed significantly both from controls ($P < 0.05$) and from patients with small lesions ($P < 0.01$) (Fig. 11). Patients with small lesions showed no significant difference from controls ($P = 0.29$).

TVA Fits
As anticipated, the spatial bias scores we derived from equation (4) were closely related to equivalent scores (equation 3) obtained by a full fit of TVA to each participant's data (see http://www.psy.ku.dk/cvc/TVA/TVAProgram.htm) ($R^2 = 0.82$, $P < 0.01$). There was an intermediate correlation between α' (equation 6) and values of α obtained by a full TVA fit (equation 5) ($R^2 = 0.46$, $P < 0.01$). The greatest discrepancies between α' and α occurred in four patients with very strong spatial bias. Partialling out spatial bias vastly improved the correlation between α' and α ($R^2 = 0.74$, $P < 0.01$), while leaving a substantial correlation between lesion volume and α' ($R^2 = 0.37$, $P < 0.01$, all patients combined).

Discussion

Spatial Bias
Our data show a clear dissociation between processing speed and spatial bias. While speed is impaired specifically by TPJ lesions, spatial bias is predicted simply by the volume of tissue damaged in either parietal or frontal cortex.

Parietal lesions are often emphasized in discussions of attentional bias. Our data, however, agree with many others in showing that extinction-like results can follow a wide variety of cortical and subcortical lesions (Bender, 1952; Vallar *et al.*, 1994). Even when a peripheral nerve is damaged, there can be extinction of touch on the affected part of the body — such a touch is felt when it occurs alone, but not when it is accompanied by simultaneous touch on another, unaffected body part (Bender, 1952). According to the biased competition model, objects compete for representation in many parts of sensorimotor network. As outlined earlier, a key principle is
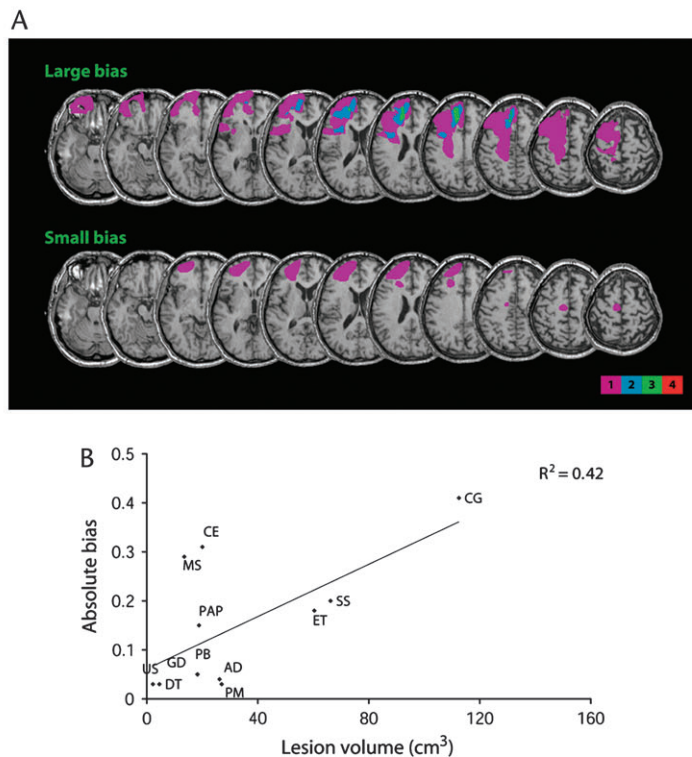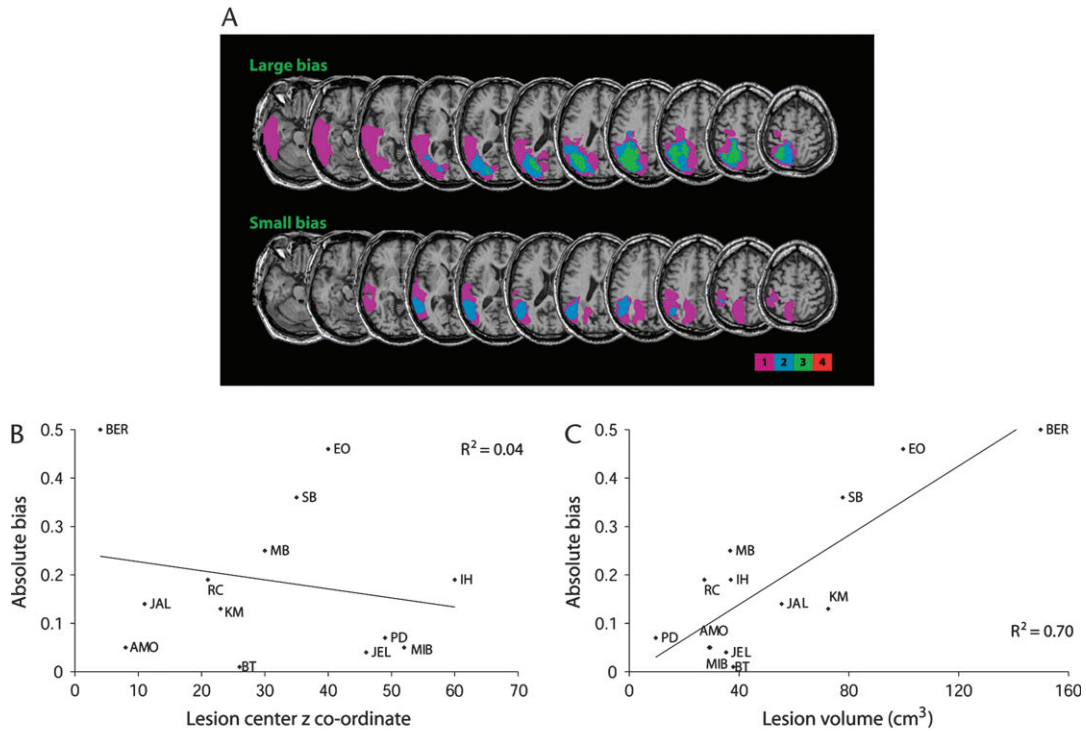
Figure 9. Absolute spatial bias in parietal patients. (*A*) Lesion overlay diagrams of the four patients with largest bias (upper panel) (three patients with right lesions and one with left lesion) and four patients with smallest bias (lower panel) (three patients with left lesions and one with right lesion). Conventions as Figure 6. (*B*) Relationship between absolute bias and z coordinate of lesion center of mass. (*C*) Relationship between absolute bias and lesion volume.

Figure 10. Absolute spatial bias in frontal patients. (*A*) Lesion overlay diagrams of the four patients with largest bias (upper panel) (all four patients with right lesions) and four patients with smallest bias (lower panel) (three patients with left lesions and one with right lesion). Conventions as Figure 6. (*B*) Relationship between absolute bias and lesion volume.

integration: weakening an object's representation in any one part of the network should produce a global processing bias against that object (Duncan, 1996; Duncan *et al.*, 1997). In line with our effects of lesion volume, furthermore, more extensive damage might be expected to produce a stronger attentional imbalance.

In the great majority of cases, the bias in our patients favored the ipsilesional side (Fig. 8). This is the result we should expect
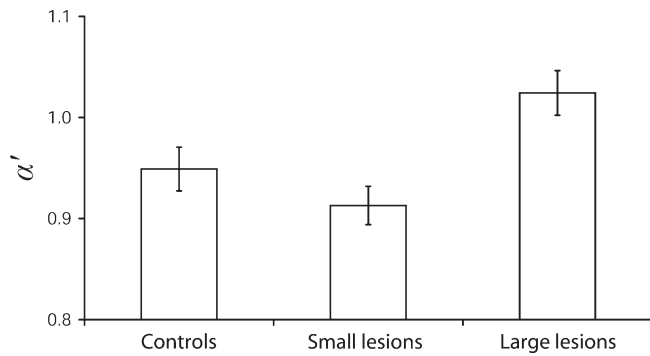
Figure 11. Mean (± SE) α′ for controls and combined parietal and frontal patients split by lesion size. The small-lesion group has four parietal and nine frontal patients. The large-lesion group has nine parietal and three frontal patients.

wherever damage selectively weakens the representation of the opposite side of space. In parietal cortex, single-unit recording in the monkey shows a preponderance of spatial receptive fields opposite to the recording location (e.g. Anderson *et al.*, 1990). For animals carrying out spatial tasks, the same has also been reported for prefrontal cortex (e.g. Funahashi *et al.*, 1989; Rainer *et al.*, 1998a). Occasional patients, however, show a paradoxical opposite bias, with an apparent preference for the contralesional field (Fig. 8; see also Duncan *et al.*, 1999). Possibly, this reflects deliberate, top-down compensation in some patients who have learned to recognize their underlying contralesional deficit (Humphreys *et al.*, 1996). In some cases, too, paradoxical bias may reflect damage to systems whose primary role is inhibiting unwanted actions directed to the opposite side (Guitton *et al.*, 1985); in this case, a bias against ipsilesional space would reflect contralesional disinhibition. More work is needed to show whether paradoxical bias is associated with particular lesion characteristics.

At least in our data, there was no strong effect of lesion side. This contrasts with unilateral neglect, well known to be stronger and more persistent after right hemisphere lesions (Bisiach and Vallar, 1988). Neglect — manifest as a gross clinical failure to deal with the contralateral side of space — was weak or absent in our patients. It is common in acute brain damage, but usually shows rapid recovery (Stone *et al.*, 1992). As others have suggested, full-blown neglect may require a combination of spatial and nonspatial deficits, e.g disordered arousal (Karnath, 1988; Robertson, 2001; Husain and Rorden, 2003). Though spatial bias is surely a component of the disorder, on its own it may not be strongly associated with right hemisphere lesions.

Top-down Control

Although overall impairments in top-down control were not seen in either patient group relative to controls, significant correlations between lesion volume and top-down control scores were independently seen in each group. A subsequent analysis pooling across the two patient groups showed that the patients with larger lesions were significantly impaired relative to both controls and patients with smaller lesions. Our results suggest that both parietal and frontal cortex are involved in attentional weighting by task relevance (see also Rossi *et al.*, 1999; Gehring and Knight, 2002; Friedman-Hill *et al.*, 2003).

Biased competition accounts frequently emphasize the control role of prefrontal cortex (Desimone and Duncan, 1995; Miller and Cohen, 2001). As shown by many single cell studies, frontal neurons do not have fixed response properties. Instead

they adapt to code information that describes a current task — its inputs, outputs, working memory contents, rewards and so on (Duncan, 2001; Rainer *et al.*, 1998b; Sakagami and Niki, 1994). According to the biased competition view, this frontal representation supports coding of task-related information in many other parts of the brain (Duncan, 2001; Miller and Cohen, 2001). In visual attention studies, for example, the proposal is that task instructions set up a sustained frontal signal indicating the category of objects to be selected (e.g. objects in a certain color, as here, or objects in a certain location, as in spatial attention studies). In many parts of the visual system, this frontal signal supports the firing of target-related cells. When a visual display is presented, these sustained signals give a competitive advantage to objects matching the target category. In TVA, this would correspond to an increase in target attentional weights.

Our data suggest that parietal cortex may play a somewhat paralell role in top-down control. In fact, single cell studies document highly similar properties in frontal and parietal regions (Chafee and Goldman-Rakic, 1998). Similar activation profiles are also common in neuroimaging (Cabeza and Nyberg, 2000). While many regions of parietal cortex are thought to be specialized for spatial functions, nonspatial information can also be represented when it is relevant to a monkey's task (Toth and Assad, 2002). Again it seems possible that parts of parietal cortex have rather adaptable properties, with the ability to focus on a broad variety of task-relevant information.

A number of neuroimaging studies have specifically examined parietal and frontal responses to attentional instruction cues. In these studies, a cue tells the subject to prepare for stimuli in a particular location, or for objects with certain features or properties. Certainly, frontal responses to such cues are common. In line with our finding that control deficits are associated more with lesion volume than with any specific region of frontal damage, cue-related activity is found across several regions of frontal cortex (Hopfinger *et al.*, 2000; Shulman and Corbetta, 2004). As expected from the role of parietal cortex in spatial processing, several studies have also shown parietal activity linked to spatial cues (Kastner *et al.*, 1999; Corbetta *et al.*, 2002). Again, though, there is also evidence for nonspatial responses (Shulman and Corbetta, 2004). A recent study (Giesbrecht *et al.*, 2003), for example, found much the same regions of superior frontal cortex and posterior parietal cortex to be activated by spatial and color cues. Also in line with our findings on lesion volume, cue responses are strong in the intraparietal sulcus and superior parietal lobule (Corbetta *et al.*, 2002), but they also occur in the inferior parietal lobule, temporoparietal junction and superior temporal gyrus (Corbetta *et al.*, 2002; Hopfinger *et al.*, 2000). More work is needed to define the exact contributions of frontal and parietal mechanisms. Meanwhile, the data suggest that both play an important part in top-down attentional control.

From the biased competition view, control functions are implemented through support of target-related responses in much of the visual system (Desimone and Duncan, 1995). In both monkey and human studies, sustained responses following attentional instruction cues have been described in occipito-temporal as well as frontal and parietal cortex (e.g. Chelazzi *et al.*, 1993; Kastner *et al.*, 1999). In the monkey, occipitotemporal lesions can increase the effects of visual distraction, suggesting impaired top-down control (De Weerd *et al.*, 1999). In the human, more data are needed to examine control deficits from lesions outside frontal and parietal cortex.

Part 3: VSTM Capacity

According to TVA, one further parameter limits performance in tasks of the sort we have used. When a display element is identified (equation 1), its identity can be entered into VSTM, making it available for report. Accordingly, display elements race to be processed, either until processing terminates (when the display is followed by a backward mask, or decays post-offset), or until VSTM is filled. The capacity of VSTM, K, is thus the maximum number of letters than can be reported following a single brief display; for normal observers, it typically ranges between 3 and 5.

One simple procedure would be to estimate K as the maximum number of letters ever reported on a single trial. Obviously, the display must contain more than K letters. Exposure duration is less important since, empirically, the maximum tends to be fairly constant across a broad range of durations. We used data from the 6T displays described in Part 2. In practice, TVA's procedure is more complex than simply finding the maximum number of letters ever reported (Bundesen, 1990; Duncan *et al.*, 1999). Data fits are generally improved by allowing non-integer K values, interpreted as probability mixtures. An estimate of 3.2, for example, is interpreted as a value of 3.0 with a probability of 0.8, and a value of 4.0 with a probability of 0.2. Here we approximate TVA's procedure without detailed model fitting. If T_n is the proportion of trials with n letters reported and m is the maximum number ever reported by a given participant, then the estimate of VSTM capacity K' is

$$K' = \left(m \times \frac{T_m}{T_m + T_{m-1}} \right) + \left((m-1) \times \frac{T_{m-1}}{T_m + T_{m-1}} \right) \qquad (7)$$

For comparison with VSTM scores, we also administered standard tests of digit and spatial working memory.

Materials and Methods

VSTM
To estimate VSTM capacity, we used data from the 6T trials of the partial report task described in Part 2.

Working Memory
Measures of working memory span were adapted from the 'forward' versions of digit span and Corsi blocks tasks in the WMS-III (Wechsler, 1997). Our modifications aimed to provide a more sensitive measure of span by running 15 trials of each task. On the first trial the span list consisted of three items; after each trial, sequence length was increased by one item if recall was correct and decreased by one item if it was not. The score was mean sequence length over the last 10 trials.

Results

VSTM
As described in equation (7), the estimate of VSTM capacity, K', derives from the distribution of scores (number of letters reported) on 6T trials. Illustrative distributions appear in Figure 12. Specifically, K', like the TVA measure of K, is the average of the participant's best and second-best scores (for Fig. 12*A*, 5 and 4; for Fig. 12*B,C*, 3 and 2), weighted by their relative frequency.

Parietal Patients.. K′ estimates for each participant appear in Table 2. Distributions across participants appear in Figure 13*A,B* (controls and parietal patients respectively). An ANOVA showed
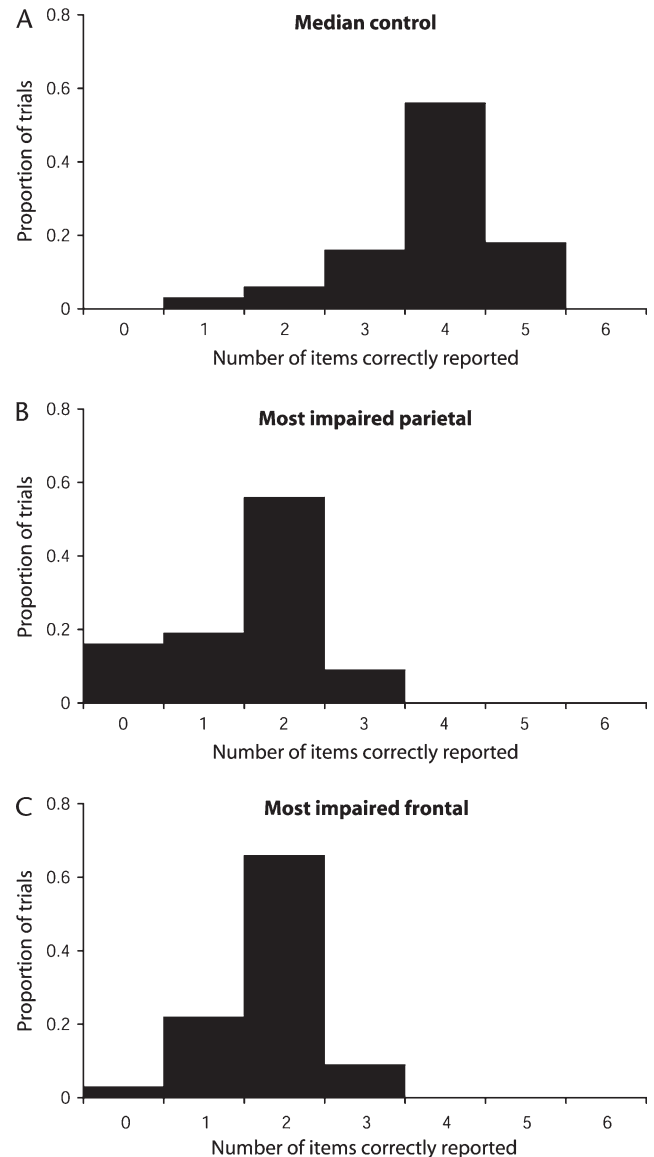

Figure 12. Data for three illustrative participants in six-target trials. (*A*) Control (AJ) with median *K′*. (*B*) Lowest *K′* parietal patient (SB). (*C*) Lowest *K′* frontal patient (CE). Each figure shows proportion of trials with 0, 1, 2, 3, 4, 5, 6 letters correctly reported.

no significant difference between left and right parietal groups [$F(1,12) = 0.52$]. Combined left and right patients, however, were significantly impaired relative to controls [$F(1,21) = 13.66$, $P < 0.01$].

Lesions of the four best and four worst patients are compared in Figure 14*A*. As for speed in Part 1, the results suggest that VSTM impairment is specifically associated with more ventral lesions, in the region of the TPJ. Again this is confirmed by regression analysis: K' was strongly correlated with lesion *z*-level, $R^2 = 0.38$, $P < 0.05$ (Fig. 14*B*), but not with lesion volume, $R^2 = 0.11$ (Fig. 14*C*). To summarize, K', like v_i in Part 1, was impaired in parietal patients, in particular by lesions in the region of the TPJ.

Frontal Patients. K′ estimates for left and right frontal patients did not differ significantly [$F(1,10) = 2.55$]. Neither did frontal patients as a whole differ from controls [$F(1,21) = 3.21$], though
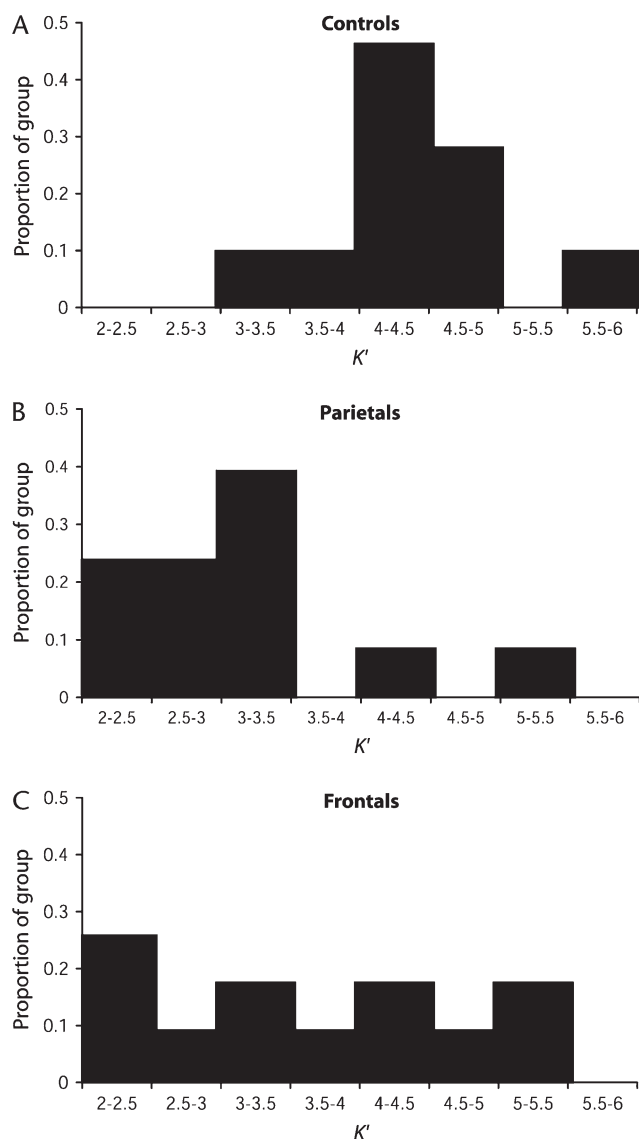
Figure 13. Distributions of K' for control participants (A), patients with parietal lesions (B) and patients with frontal lobe lesions (C).

certainly some patients had K' values below the control distribution (Fig. 13C). Further analyses in the patient group showed that K' was not significantly related to lesion volume ($R^2 = 0.10$). To summarize, any K' deficit in frontal patients was modest, and not significant in the group as a whole.

VSTM and Processing Speed. The similar profiles of impairment in v_i and K' prompts the question of their relationship. A significant correlation was found in the control group ($R^2 = 0.48$, $P < 0.05$), but not in parietal patients ($R^2 = 0.05$) or in frontal patients ($R^2 = 0.14$).

TVA Fits. As anticipated, the scores we derived for K' were closely related to K scores obtained by a full fit of TVA to each participant's data ($R^2 = 0.87$).

Working Memory

Mean digit span was 7.3 in controls, 6.6 and 6.9 respectively for left and right parietals, and 7.6 and 6.6 respectively for left and right frontals. Neither combined parietals [$F(1,19) = 1.85$] nor

combined frontals [$F(1,18) = 0.24$] differed significantly from controls. Mean spatial span was 5.6 in controls, 5.4 and 5.5 respectively in left and right parietals, and 5.9 and 5.3 respectively in left and right frontals. Again, neither combined parietals [$F(1,19) = 0.1$] nor combined frontals [$F(1,18) = 0.01$] differed significantly from controls. In the parietal group, both digit span ($R^2 = 0.41$, $P < 0.05$) and spatial span ($R^2 = 0.21$, $P = 0.05$) showed a tendency to correlate with K'. Neither span, however, showed a significant association with lesion z-level ($R^2 = 0.07$ for digit span, $R^2 = 0.13$ for spatial span).

Discussion

Similar to results for processing speed, we found reduced capacity of VSTM to be specifically associated with lesions in the region of the TPJ. In the frontal lobe group, we found some patients with low VSTM capacity, but no significant deficit in the group as a whole.

Our data do not definitively show whether reduced K' reflects a general reduction in working memory. On the one hand, K' scores tended to correlated with both digit and spatial span. On the other hand, reduced spans were not specifically associated with TPJ lesions. More work is needed to show how VSTM — the maximum number of objects perceived in a single, brief display — relates to more conventional working memory limitations.

The association of VSTM deficits with ventral lesions may relate to the clinical phenomenon of Bálint's syndrome (Bálint, 1995 [1909]), typically associated with bilateral parietal lobe lesions. Conventionally, one component of Bálint's sydrome is 'simultanagnosia', a specific impairment in attending to more than one visual input at once. In principle, TVA could model a pure simultanagnosia by setting the K value to one. While single-element processing would be normal, it would be impossible to see more than one display element at a time. In practice, there may be few patients with truly preserved single-element processing. In one typical case, for example, we recently found major deficits in simple processing speed for a single, foveal input (Duncan *et al.*, 2003). In the literature, indeed, we know of only one case with unambiguous evidence of normal single-element processing (Coslett and Saffran, 1991). In light of the present data, it may be important that, in this one patient, lesions were rather ventral, affecting occipitotemporal cortex in both hemispheres.

In a recent imaging study, VSTM has been linked to a region in the intraparietal sulcus (Todd and Marois, 2004). In this region, activation increased with the number of objects displayed to a maximum of 3–4, matching a behavioral measure of VSTM capacity. For only three of our patients, however, did the lesion overlap with the peak activation reported by Todd and Marois (2004). More patients would be needed to assess the effects of damage to this region.

Conclusion

Despite their physiological plausibility (Desimone and Duncan, 1995) and success in accounting for normal data (Bundesen, 1990), competitive parallel models have been little applied in the neuropsychology of attentional deficits. To guide our work we used TVA and the closely related ideas of biased competition. We analyzed deficits in speed of visual processing, spatial bias, top-down control and VSTM.

The results contain a number of surprises. The deficits specifically associated with parietal lesions are not spatial.
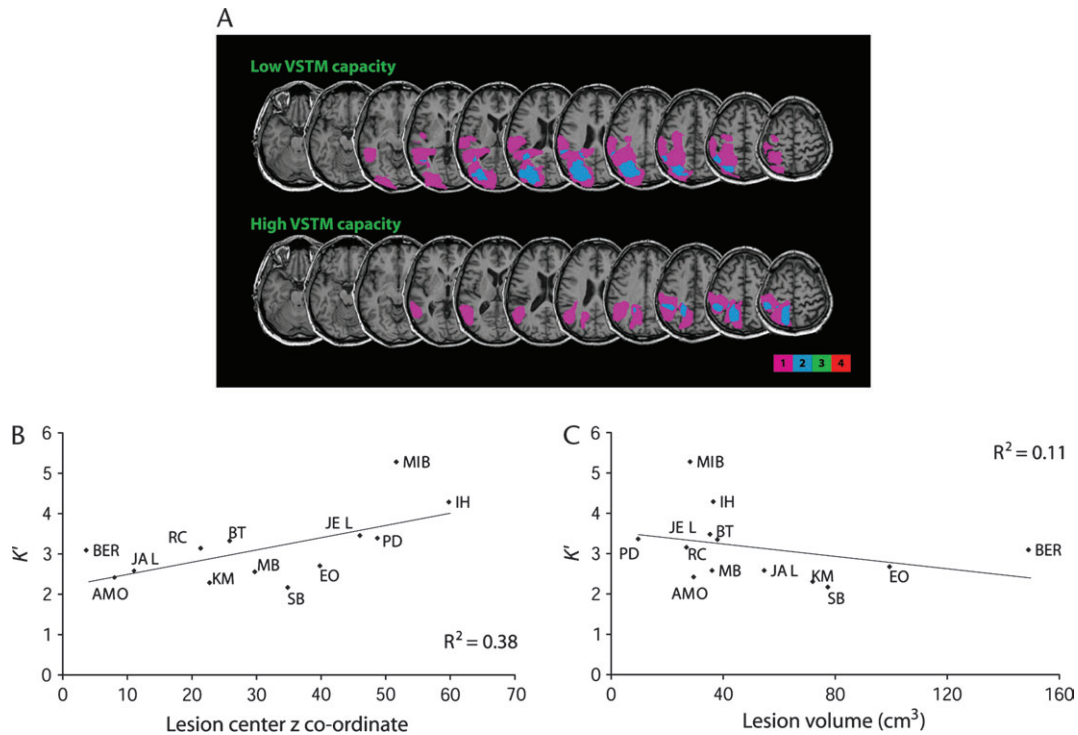
Figure 14. VSTM capacity in parietal patients. (*A*) Lesion overlay diagrams of the four patients with lowest *K′* (upper panel) (all patients had left lesions) and four patients with highest *K′* (lower panel) (three left lesions and one right lesion). Conventions as Figure 6. (*B*) Relationship between *K′* and *z* coordinate of lesion center of mass. (*C*) Relationship between *K′* and lesion volume.

Instead, lesions around the TPJ produce deficits in nonspatial aspects of processing — both speed of processing and capacity of VSTM. Spatial bias, in contrast, is associated with parietal, frontal or occipitotemporal (Duncan *et al.*, 2003) lesions, and is largely predicted by simple lesion volume. Neither do we find a specific association between frontal lesions and deficits in top-down control. Instead, again, control deficits are associated with simple lesion volume, with similar results for parietal and frontal cortex. For parietal and frontal regions, the picture is one of somewhat distinct, but also somewhat parallel contributions to competitive visual processing.

Notes

Address correspondence to John Duncan, MRC Cognition and Brain Sciences Unit, 15 Chaucer Road, Cambridge CB2 2EF, UK. Email: john.duncan@mrc-cbu.cam.ac.uk.

References

Anderson RA, Asanuma C, Essick G, Siegel RM (1990) Corticocortical connections of anatomically and physiologically defined subdivisions within the inferior parietal lobule. J Comp Neurol 296:65–113.

Baddeley A, Emslie H, Nimmo Smith I (1993) The Spot-the-Word test: a robust estimate of verbal intelligence based on lexical decision. Br J Clin Psychol 32:55–65.

Bálint R (translated by Harvey, M) (1995 [1909]) Psychic paralysis of gaze optic ataxia and spatial disorder of attention. Cogn Neuro-psychol 12:265–281.

Beck DM, Rees G, Frith CD, Lavie N (2001) Neural correlates of change detection and change blindness. Nat Neurosci 4:645–650.

Bender MB (1952) Disorders in perception. Springfield, IL: Charles C. Thomas.

Bisiach E, Vallar G (1988) Hemineglect in humans. In: Handbook of neuropsychology, Vol. 1 (Boller F, Grafman J, eds), pp. 195–222. Amsterdam: Elsevier.

Brett M, Leff AP, Rorden C, Ashburner J (2001) Spatial normalization of brain images with focal lesions using cost function masking. Neuro-image 14:486–500.

British Society of Audiology (1981) Recommended procedures for pure-tone audiometry using a manually operated instrument. Br J Audiol 15:213–216.

Bundesen C (1990) A theory of visual attention. Psychol Rev 97:523–547.

Bundesen C, Shibuya H, Larsen A (1985) Visual selection from multielement displays: a model for partial report. In: Attention and performance XI (Posner MI, Marin O, eds), pp. 631–649. Hillsdale, NJ: Erlbaum.

Cabeza R, Nyberg L (2000) Imaging cognition. II. An empirical review of 275 PET and fMRI studies. J Cogn Neurosci 12:1–47.

Chafee MV, Goldman-Rakic PS (1998) Matching patterns of activity in primate prefrontal area 8a and parietal area 7ip neurons during a spatial working memory task. J Neurophysiol 79:2919–2940.

Chelazzi L, Miller EK, Duncan J, Desimone R (1993) A neural basis for visual search in inferior temporal cortex. Nature 363:345–347.

Cohen L, Lehericy S, Chochon F, Lemer C, Rivaud S, Dehaene S (2002) Language-specific tuning of visual cortex? Functional properties of the Visual Word Form Area. Brain 125:1054–1069.

Corbetta M, Miezin FM, Dobmeyer S, Shulman GL, Petersen SE (1990) Attentional modulation of neural processing of shape color and velocity in humans. Science 248:1556–1559.

Corbetta M, Kincade MJ, Ollinger JM, McAvoy MP, Shulman GL (2000) Voluntary orienting is dissociated from target detection in human posterior parietal cortex. Nature Neurosci 3:292–297.

Corbetta M, Kincade MJ, Shulman GL (2002) Neural systems of visual orienting and thier relationship to spatial working memory. J Cogn Neurosci 14:508–523.

Coslett HB, Saffran E (1991) Simultanagnosia. To see but not two see. Brain 114:1523–1545.

Desimone R, Duncan J (1995) Neural mechanisms of selective visual attention. Annu Rev Neurosci 18:193–222.

DeWeerd P, Peralta MR, Desimone R, Ungerleider LG (1999). Loss of attentional stimulus selection after extrastriate cortical lesions in macaques. Nat Neurosci 2:753–758.

Downar J, Crawley AP, Mikulis DJ, Davis KD (2000) A multimodal cortical network for the detection of changes in the sensory environment. Nat Neurosci 3:277–283.

Downar J, Crawley AP, Mikulis DJ, Davis KD (2001) The effect of task relevance on the cortical response to changes in visual and auditory stimuli: an event-related fMRI study. Neuroimage 14:1256-1267.

Duncan J (1984) Selective attention and the organization of visual information. J Exp Psychol Gen 113:501–517.

Duncan J (1996) Cooperating brain systems in selective perception and action. In: Attention and performance XVI (Inui T, McClelland JL, eds), pp. 549–578. Cambridge, MA: MIT Press.

Duncan J (2001) An adaptive coding model of neural function in prefrontal cortex. Nat Rev Neurosci 2:820–829.

Duncan J, Humphreys GW, Ward R (1997) Competitive brain activity in visual attention. Curr Opin Neurobiol 7:255–261.

Duncan J, Bundesen C, Chavda S, Olson A, Humphreys GW, Shibuya H (1999) Systematic analysis of deficits in visual attention. J Exp Psychol 128:450–478.

Duncan J, Bundesen C, Olson A, Humphreys GW, Ward R, Kyllingsbæk S, van Raamsdonk M, Rorden C, Chavda S (2003) Attentional functions in dorsal and ventral simultanagnosia. Cogn Neuropsychol 20:675–701.

Fitts PM, Deininger RL (1954) S-R compatibility: Correspondence among paired elements within stimulus and response codes. J Exp Psychol 48:483–492.

Friedman-Hill SR, Robertson LC, Desimone R, Ungerleider LG (2003) Posterior parietal cortex and the filtering of distractors. Proc Natl Acad Sci USA 7:4263–4268.

Funahashi S, Bruce CJ, Goldman-Rakic PS (1989) Mnemonic coding of visual space in the monkey's dorsolateral prefrontal cortex. J Neurophysiol 61:331–349.

Gaffan D, Hornak J (1997) Visual neglect in the monkey: representation and disconnection. Brain 120:1647-1657.

Gehring WJ, Knight RT (2002) Lateral prefrontal damage affects processing selection but not attention switching. Cogn Brain Res 13:267–279.

Giesbrecht B, Woldorff MG, Song AW, Mangun GR (2003) Neural mechanisms of top-down control during spatial and feature attention. Neuroimage 19:496–512.

Guitton D, Buchtel HA, Douglas RM (1985) Frontal lobe lesions in man cause difficulties in suppressing reflexive glances and in generating goal-directed saccades. Exp Brain Res 58:455–472.

Hopfinger JB, Buonocore MH, Mangun GR (2000) The neural mechanisms of top-down attentional control. Nat Neurosci 3:284–291.

Humphreys GW, Boucart M, Datar V, Riddoch MJ (1996) Processing fragmented forms and strategic control of orienting in visual neglect. Cogn Neuropsychol 13:177–203.

Husain M, Rorden C (2003) Non-spatially lateralized mechanisms in hemispatial neglect. Nat Rev Neurosci 4:26–36.

Kanwisher N, McDermott J, Chun MM (1997) The fusiform face area: a module in human extrastriate cortex specialized for face perception. J Neurosci 17:4302–4311.

Karnath H-O (1988) Deficits in attention in acute and recovered visual hemi-neglect. Neuropsychologia 26:27–43.

Kastner S, Pinsk MA, De Weerd P, Desimone R, Ungerleider LG (1999) Increased activity in human visual cortex during directed attention in the absence of visual stimulation. Neuron 22:751–761.

Linden DE, Prvulovic D, Formisano E, Vollinger M, Zanella FE, Goebel R, Dierks T (1999) The functional neuroanatomy of target detection: an fMRI study of visual and auditory oddball tasks. Cereb Cortex 9:815–823.

Malach R, Reppas JB, Benson RR, Kwong KK, Jiang H, Kennedy WA, Ledden PJ, Brady TJ, Rosen BR, Tootell RB (1995) Object-related activity revealed by functional magnetic resonance imaging in human occipital cortex. Proc Natl Acad Sci USA 92:8135-8139.

Marois R, Leung H-C, Gore JC (2000). A stimulus-driven approach to object identity and location processing in the human brain. Neuron 25:717–728.

Miller EK, Cohen JD (2001) An integrative theory of prefrontal cortex function. Annu Rev Neurosci 24:167–202.

Rainer G, Asaad WF, Miller EK (1998a) Memory fields of neurons in the primate prefrontal cortex. Proc Natl Acad Sci USA 95: 15008-15013.

Rainer G, Asaad WF, Miller EK (1998b) Selective representation of relevant information by neurons in the primate prefrontal cortex. Nature 393:577–579.

Robertson IH (2001) Do we need 'lateral' in unilateral neglect? Spatially nonselective attention deficits in unilateral neglect and their implications for rehabilitation. Neuroimage 14:S85–S90.

Rorden C, Brett M (2000) Stereotaxic display of brain lesions. Behav Neurol 12:191–200.

Rossi AF, Rotter PS, Desimone R, Ungerleider LG (1999) Prefrontal lesions produce impairments in feature-cued attention. Soc Neurosci Abstr 25:3.

Rumelhart DE (1970) A multicomponent theory of the perception of briefly exposed visual displays. J Math Psychol 7:191–218.

Sakagami M, Niki H (1994) Encoding of behavioral significance of visual stimuli by primate prefrontal neurons: relation to relevant task conditions. Exp Brain Res 97:423–436.

Samuelsson H, Jensen C, Ekholm S, Naver H, Blomstrand C (1997) Anatomical and neurological correlates of acute and chronic visuospatial neglect following right hemisphere stroke. Cortex 33:271–285.

Shulman GL, Corbetta M (2004) Endogenous and stimulus-driven mechanisms of task control. In: Attention and performance. XX. Functional neuroimaging of visual cognition (Kanwisher N, Duncan J, eds), pp. 345–362. Oxford: Oxford University Press.

Soltani M, Knight RT (2000) Neural origins of the P300. Crit Rev Neurobiol 14:199–224.

Sperling G (1960) The information available in brief visual presentations. Psychol Monogr 48:no. 498.

Sternberg S (1969) The discovery of processing stages: extensions of Donders' method. In: Attention and performance II (Koster WG, ed.), pp. 276-315. Amsterdam: North-Holland.

Stone SP, Patel P, Greenwood RJ, Halligan PW (1992) Measuring visual neglect in acute stroke and predicting its recovery: the visual neglect recovery index. J Neurol Neurosurg Psychiatry 55:431–436.

Todd JJ, Marois R (2004) Capacity limit of visual short-term memory in human posterior parietal cortex. Nature 428:751–754.

Toth LJ, Assad JA (2002) Dynamic coding of behaviourally relevant stimuli in parietal cortex. Nature 415:165–168.

Tzourio-Mazoyer N, Landeau B, Papathanassiou D, Crivello F, Etard O, Delcroix N, Mazoyer B, Joliot M (2002) Automated anatomical labeling of activations in SPM using a macroscopic anatomical parcellation of the MNI MRI single subject brain. Neuroimage 15:273–289.

Vallar G, Rusconi ML, Bignamini L, Geminiani G, Perani D (1994) Anatomical correlates of visual and tactile extinction in humans: A clinical CT scan study. J Neurol Neurosurg Psychiatry 57:464–470.

Ward R, Goodrich S, Driver J (1994) Grouping reduces visual extinction: neuropsychological evidence for weight-linkage in visual selection. Visual Cogn 1:101–129.

Wechsler D (1997) Wechsler Memory Scale, 3rd UK edn. London: The Psychological Corporation.

Weintraub S, Mesulam MM (1985) Mental state assessment of young and elderly adults in behavioral neurology. In: Principles of behavioural neurology (Mesulam MM, ed.), pp. 71-123. Philadelphia, PA: Davis FA.

Wilson BA, Cockburn J, Halligan PW (1987) Behavioural inattention test. Fareham UK: Thames Valley Test Company.